

Central European Journal of Chemistry

Structural characterization of Th-doped TiO₂ photocatalyst and its extension of response to solar light for photocatalytic oxidation of oryzalin pesticide: a comparative study

Research Article

L. Gomathi Devi*, B. Narasimha Murthy

Department of Chemistry, Bangalore University, Bangalore – 560 001, India

Received 25 June 2008; Accepted 15 October 2008

Abstract: The degradation efficiency of Th-doped TiO₂ / TiO₂ photocatalysts were investigated under UV and solar light illumination. The model compound chosen for the study was Oryzalin (OZ). Doping of inner transition metal ion Th was intended to modify the electronic properties of TiO₂. The Th-doped TiO₂ were synthesized by incorporating 0.02, 0.04, 0.06, and 0.1 atom percentage of Th into the TiO₂ lattice by solid-state reaction. The stochiometry of the prepared samples is Ti_{1,x}Th_xO₂, where 'x' is the percentage of Th. The samples were characterized by UV-Visible absorption, UV-Visible -Diffused reflectance spectra, Scanning Electron Microscopy (SEM), Energy Dispersive X-ray Analysis (EDX) and X-ray Diffraction (XRD). The pore size and surface area of these samples were studied by Brunauer, Emmett and Teller (BET) adsorption method. It was found that metal ion doping at various percentage compositions enables a large shift in the absorption band of the TiO₂ towards visible light region. This is due to the formation of various mid band gaps at 2.84 eV, 2.804 eV, 2.66 eV, and 2.55 eV. The extent of degradation of the pesticide was followed by UV-Visible spectroscopy and GC-MS methods. Based on the spectral analysis, the probable degradation reaction mechanism for OZ is proposed. These results indicate that Th-doped TiO₂ with the modified electronic properties is a good catalyst under solar light irradiation. But these particles show marginal variation in rates under UV-illumination. All the photodegradation reactions follow the first order kinetics.

Keywords: Th-doped TiO, • Oryzalin • Photocatalysis • Mid band gaps of TiO, • Spectroscopic analysis.

© Versita Warsaw and Springer-Verlag Berlin Heidelberg.

1. Introduction

OZ is a selective pre-emergence surface applied herbicide used for the control of annual grasses and broad leaf weeds in fruit and nut trees. It inhibits the growth of germinating weed seeds by blocking cell divisions in the meristeams. OZ shows low to moderate persistence in the field. The contamination of surface water with pesticides is due to the surface runoff from agricultural activities. The concentration of these pesticides has been reported to exceed the maximum contaminant level permitted for the surface waters [1-10]. OZ is resistant to natural decomposition process; its life time in aqueous media in nature is about 20-128 days [11]. No breakdown of OZ by hydrolysis was observed at pH 5, 7, and 9 [12]. Furthermore, the natural decomposition leads to several

toxic organic intermediates which affect the immunity of the human population consuming water from polluted sources. The pesticide and its degradation reaction intermediates still persist even after passing conventional water treatment procedure [6,7]. The present wastewater treatment is ineffective in removing these contaminants. These compounds are well known carcinogenic and mutagenic in nature [8,11].

 ${
m TiO_2}$ is a very suitable photocatalyst because of its low cost, chemical stability, non-toxic nature, optical and electronic properties [13-15]. However due to its high band-gap energy, ${
m TiO_2}$ utilizes only a very small fraction of the solar spectrum and thus doping with transition metals have been so far employed to extend the light absorption to the visible region [13-18]. The presence of foreign metal species in ${
m TiO_2}$ nanoparticles showed many controversial

results which are reported in literature. Hoffmann et al. [19], found that doping quantum-sized TiO₂ with Fe³⁺, Mo⁵⁺, Ru³⁺, Os³⁺, Rh⁵⁺, and V⁴⁺ at 0.1-0.5% significantly enhanced the photoreactivity for the oxidation of CHCl₃ and the reduction of CCI₄, whereas doping of Co³⁺ and Al3+ decreased the photoreactivity. W. Lee et al. found that the photocatalytic activity of TiO2 towards the oxidation of 1,4-dichlorobenzene was improved significantly by introduction of WO₃ and MoO₃ [20,21] and a beneficial influence of tungsten was found for the photodegradation of 4-nitrophenol [22,23]. Cr3+is reported to significantly reduce the photocatalytic performances of TiO₂ [16,24]. But Apno et al. report that Cr and V ion doped TiO, has shown photocatalytic reactivity three to four times higher than TiO, for the decomposition of NO under solar beam irradiation [25]. The method of doping and the nature of the reaction obviously determine the properties of the catalyst. To our knowledge, doping of a metal ion with 5f electronic configuration (Th) into the TiO₂ matrix has not been reported.

This paper concentrates on (i) the preparation of Th-doped ${\rm TiO}_2$ with various percentages raging from 0.02 to 0.1, (ii) material characterization of photocatalysts, (iii) comparative study of photocatalytic activities under UV and solar light illumination, (iv) spectroscopic analysis of degradation reaction intermediates, and (v) proposal of degradation reaction mechanism.

2. Experimental Procedures

2.1 Reagents

Titanium(IV) Chloride ($TiCl_4 \ge 99.9\%$) is obtained from Merck Chemicals Ltd, $Th(NO_3)_4$ (99%) from Sisco-Chem Industries, Bombay. NH₄OH (25-28%), HCI (37%), (NH₄)₂S₂O₈ (98%) and NaOH (97%) were from Sd Fine chemicals and used as supplied. Double distilled water was used for all the experiments. OZ is an organosulphur pesticide which is obtained from M/s. Bayer (India) Ltd. (pure technical grade of 97.8%) and used as received. The molecular weight of the pesticide is 346.36 and its molecular formula is $C_{12}H_{18}N_4O_6S$, (3, 5-dinitro-N⁴, N⁴-dipropylsulfanilamide).

$$\begin{array}{c|c} H & O & NO_2 \\ H & S & CH_2 - CH_2 - CH_3 \\ \hline & NO_2 & CH_2 - CH_2 - CH_3 \\ \hline & NO_2 & CH_2 - CH_3 - CH_3 \\ \hline & NO_2 & CH_2 - CH_3 - CH_3 \\ \hline \end{array}$$

Scheme 1. Structure of OZ

2.2. Preparation of Photocatalysts

The optically pure, fine grained anatase TiO, is prepared by using sol-gel method. 100 mL of high purity TiCl, was carefully diluted by adding drop-wise to 250 mL of ice cold, well stirred double distilled water, and the resulting solution was then diluted to 500 mL. 25 mL of above diluted TiCl, was made acidic by adding around 1 mL of conc. H₂SO₄ in a beaker and diluted to 1 liter with double distilled water. Liquid ammonia was added until the pH of the diluted solution reached 7-8 in order to obtain the hydroxide of Titanium gel. The gel obtained is allowed to settle down and was washed several times to remove chloride and ammonium ions. The precipitate obtained was oven dried for 12 hours at 100°C. The oven dried TiO, was then ground in a mortar. The fine powder obtained was subjected to heat treatment at 600°C to obtain the anatase form of TiO₂ [26].

The stock solution of $Th(NO_3)_4$ was prepared by weighing 0.5050 g in 100 mL of double distilled water. From the stock solution 0.5, 1.0, 1.6, and 2.5 mL was pipetted out and mixed with 2 g of TiO_2 in an agate mortar to get 0.02, 0.04, 0.06, and 0.1% of $Th-TiO_2$. These mixtures were manually ground in a mortar. All these samples were oven dried at 100°C for 12 hours. During the process of heating, the samples were repeatedly ground for 6 times in a mortar and finally calcined at 600°C for 4.5 hours in a muffle furnace. The stoichiometry of the prepared samples is Ti_4 , Th_2O_2 where 'x' is the percentage of Th.

2.3 Instrumentation

X-ray Diffraction: The XRD patterns of the powders were recorded using Phillips powder diffractometer Pw/1050/70/76 with Cu K α radiation under the scan rate of 2° per min.

Absorption /Diffuse Reflectance Spectroscopy: The absorption and reflectance spectra were recorded by using UV-Visible Shimadzu double beam spectrophotometer 3101PC UV-VIS-NIR instrument. The spectra were recorded at room temperature in the range of 190-800 nm. The diffuse reflectance spectra were recorded with BaSO₄ as reference.

Scanning Electron Microscopy and Energy Dispersive X-ray Analysis: SEM was performed using a model JSM840 microscope operating at 25 kV on specimens upon which a thin layer of gold or carbon had been evaporated. An electron microprobe is used in EDX mode to obtain quantitative information on the amount and distribution of the metal species in the samples.

FTIR Spectral Analysis: FT-IR spectra were recorded using Nicollet IMPACT 400 D FTIR spectrometer, over the range of frequencies from 4000 - 400 cm⁻¹ using KBr as the reference sample.

Specific surface area measurements: The specific surface area measurements were determined by Digisorb 2006 surface area, pore volume analyzer-Nova Quanta Chrome Corporation instrument using multipoint BET adsorption

The photodegradation intermediates are analyzed by GC-MS-QP 5000 (Shimadzu mass spectrometer).

2.4. Photo reactor and Light Source

Both UV and solar illumination were used as energy sources in this study. The UV light source is a medium pressure mercury vapor lamp and the photon flux is found to be 7.75 mW cm⁻² as determined by ferrioxalte actinometry, the wavelength of which peaks around 340 - 370 nm. The photoreactor consists of a glass vessel with the exposure area of 153.86 cm². The photodegradation experiments were carried out by direct exposure of light into the reaction mixture. All the experiments were performed at room temperature with a constant lamp power of 125 W and a fixed distance between the photoreactor and the lamp housing (29 cm), in presence of atmospheric oxygen. Experiments using solar light were carried out from 11 am to 3 pm during the summer season in the months of April-June at Bangalore, India. The reaction vessel is placed directly under the sun. The convex lens was placed 15 cm away from the vessel in order to concentrate the intensity of the solar light and the reaction mixture was exposed to this concentrated solar light. During the course of the reaction, correction of the position of the lens was made with respect to the change in the direction of the sun for every 30 minutes. The latitude and longitudes are 12.58 N and 77.38 E respectively. The average sunlight intensity was found to be around 1200 W m-2.

2.5. Experimental procedure

For all the experiments, 3.22 mg L⁻¹ of pesticide solution was prepared with the distilled water at lab temperature (25°C). 150 mg of TiO₂ /Th-doped TiO₂ was added to the solution in presence of an oxidizing agent (ammonium persulphate). The experimental mixture is exposed to UV/Solar light for 150 minutes with constant stirring. The sample solutions are withdrawn at regular intervals for analysis and centrifuged to separate the photocatalyst particles. The volume of sample removed for each measurement was around 10 mL. The absorption spectra were recorded using UV-Visible Spectroscopy. GC-MS spectrum was recorded in order to identify the intermediates formed during the course of the reaction. The oryzalin sample was extracted in chloroform and 1 μL sample was injected (splitless). For GC-MS analysis a Thermo Electron Trace GC ultra coupled to a DSQ mass spectrometer equipped with an Alltech ECONO-CAP-EC-5 capillary column (30 m \times 0.25 mm *i.d.* \times 0.25 mm film thickness) was used. Ultra pure helium was used as the carrier gas at a flow rate of 1.2 mL min⁻¹. The injector/transfer line/trap temperatures were 220/250/200°C, respectively. Electron impact ionization was carried out at 70 eV.

3. Results and Discussion

3.1. Structural and Morphological Characterization of the Photocatalysts

Doping of inner transition metal ion Th was intended to modify the electronic properties of titanium oxide photocatalysts. It was found that metal ion doping at various percentage compositions enables a large shift in the absorption band of the titanium oxide catalysts towards the visible light regions, with different levels of effectiveness.

3.1.1. UV-Visible/Diffused reflectance spectra

The UV-Visible Diffused Reflectance spectra of different % Th-doped TiO, and anatase form of TiO, were recorded in order to calculate the band gap energy of the photocatalysts. The band gaps are calculated for all the samples by using Kubelka -Munk plots (Plot of (1-R_m)²/2R_m vs. wavelength) where R_m is ratio of relative reflectance to reflectance of non absorbing medium. Fig. 1 shows the reflectance spectra of (1-R_{...})²/2R_{...} vs. wavelength. For 0.06%, the tangent to the linear portion of the curve intersects the wavelength axis at 466 and 486 nm, therefore these wavelengths were used to calculate the band gap energy of this catalyst. Whereas for 0.04%, the tangent to the linear portion of the curve intersects the wavelength axis at 422 nm which was used to calculate the band gap energy of this catalyst. Similar calculations for other composition are listed in Table 1.

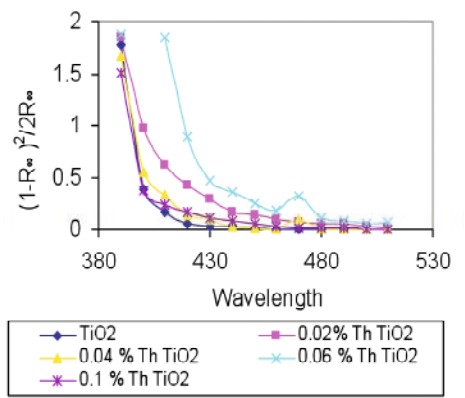


Figure 1. Kubelka-Munk plot for ${\rm TiO_2}$ and different % composition of Th-doped ${\rm TiO_2}$

In the Kubelka–Munk plot of the catalyst doped with 0.06% of Th, the steeply diminishing region around 466 nm and 486 nm corresponds to the band gap of 2.66 eV and 2.55 eV respectively. The presence of these absorption edges could be caused by the substitutional Th doping. The electronic transition in undoped TiO₂ is from O-2p valence band to Ti-3d conduction band. In the case of Th-doped TiO₂, the transition is between O-2p valence band to Th-6d-V_o level created just below the conduction band edge by 0.56 eV. Since incorporation of certain metal ions into TiO2 lattice is usually accompanied by vacancy in an oxygen site, this vacancy can be singly ionized, doubly ionized, or neutral. These new energy levels at 0.56 eV and 0.67 eV get created within the band gap. These modified catalysts should be active under visible light illumination. The magnitude of reflectance increases with increase in the % of dopant, it is probably caused due to the color change of the obtained catalysts. The color of the obtained catalysts was dependent on the amount and nature of the dopant into the TiO₂ lattice [27,28]. As the Th content increases, the absorption which results from this process is found to extend into the visible region. In addition to these energy levels, the presence of trivalent titanium cannot be ruled out and this increases the intensity of band at 486 nm (Trivalent Titania is expected to show absorption at 490 nm). Thus there is a possibility of both d-d transitions and distorted splitting. The shifting of absorption edge in the visible region is due to the distortion related modified defect centers which may have been caused due to the doping. Th-doped powders are brown in color because of Th4+ which is associated with charge transfer of electron from ligand of reducing nature to the metal. It can also originate from the f-f transition, though the f-orbital of Th is deep inside and they are largely shielded [29]. The midband gaps in Th-doped TiO, could be due to distortion related to modified defect centers caused in the process of doping. These defect states may be $\rm Th^{3^+}\text{-}V_{_{\rm O}}^{\,\, \cdot \cdot}$, and $\rm Ti^{3^+}\text{-}V_{_{\rm O}}$ (expected at 0.6 eV below the conduction band edge) [30,31]. The band gaps are calculated for all the samples from Kubelka-Munk plot [32] (Table 1).

Table 1. The band gap energy for TiO₂ and Th-doped TiO₂ samples calculated from Kubelka–Munk plot. (The steeply diminishing region of diffused reflectance spectra around 400 nm corresponds to fundamental absorption edge 3.12 eV appearing for all the samples is not mentioned in the Table)

SI. No.	Catalyst	λ (nm)	Eg (eV)
1	TiO ₂	397	3.122
2	0.02% Th TiO ₂	436	2.84
3	0.04% Th TiO ₂	422	2.804
4	0.06% Th TiO ₂	466 & 486	2.66 & 2.55
5	0.1% Th TiO ₂	410	3.02

3.1.2. UV-Visible absorption spectra

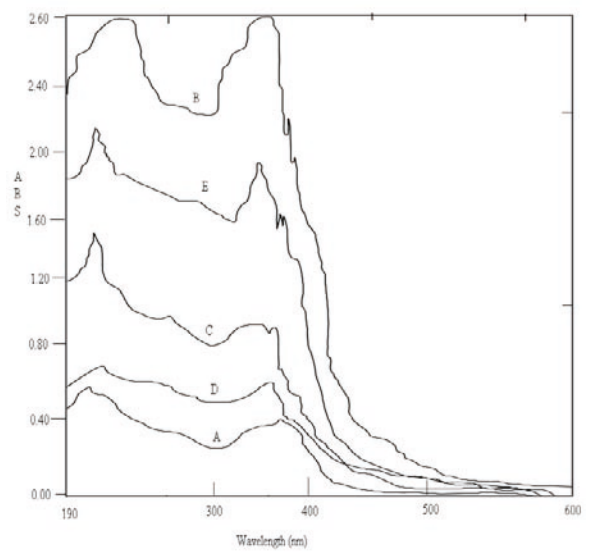
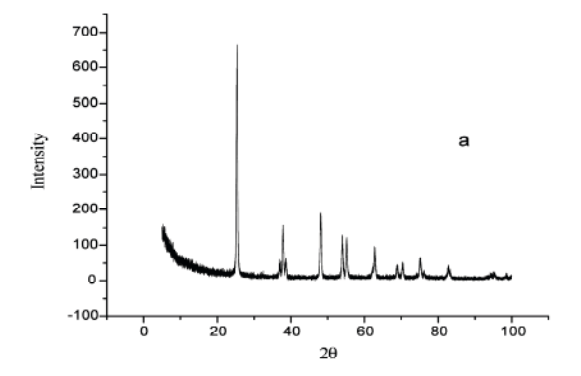
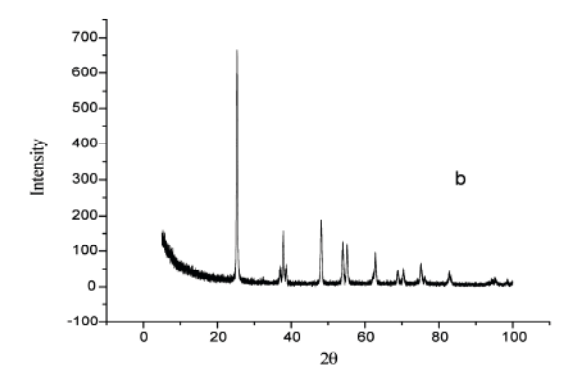


Figure 2. Absorption spectra of the photocatalysts. (A) TiO_2 , (B) 0.02% Th-doped TiO_2 (C) 0.04% Th-doped TiO_2 (D) 0.06% Th-doped TiO_2 (E) 0.1% Th-doped TiO_3

3.1.3. X-Ray Diffraction (XRD)

Fig. 3 illustrates a typical XRD spectrum of TiO, and Th-doped TiO, (different %) with 20 diffraction angles from 10° to 100°. The peaks in all the TiO₂ samples can be attributed to the anatase form of TiO, which is in agreement with the findings of N.F.M. Henry et al. [36]. These results showed that the prepared photocatalysts were of anatase structure. From the XRD data, unit cell parameters, unit cell volume, crystallite size, and density of all the TiO₂ samples were calculated (Table 2). The XRD patterns of the modified systems also show the peaks corresponding to anatase form of TiO₂. The characteristic peak corresponding to Th dopant is absent in all the XRD patterns. It is reported that in the case of metal oxides, there is a critical value of dispersion capacity. At values lower than which the oxide might become highly dispersed on the support without the formation of a separate crystalline phase [37,38]. Since no characteristic peaks corresponding to Th species is present, it can be concluded that the Th loading is below the dispersion capacity.





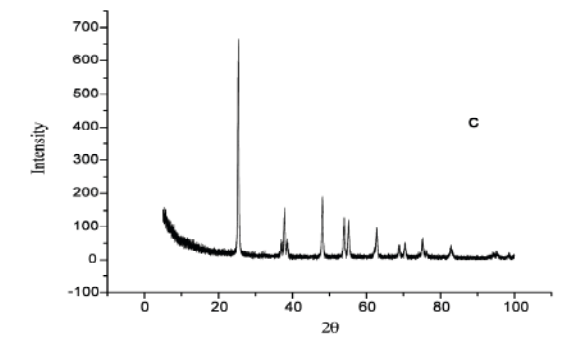


Figure 3. XRD Spectra of TiO_2 and different % of Th-doped TiO_2 . (a) TiO_2 (b) 0.06% Th-doped TiO_2 (c) 0.1% Th-doped TiO_2

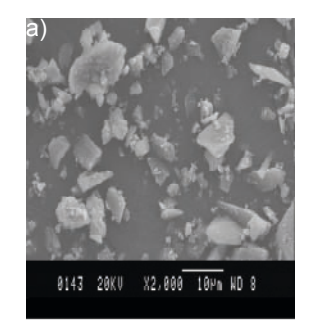
The crystallite sizes obtained from the Scherrer equation show that the crystallite size slightly increases with increase in Th content in the ${\rm TiO_2}$ lattice. The observed slight variation in the lattice parameters confirms the incorporation of Th dopant into ${\rm TiO_2}$ lattice as substitutional impurity. The change in lattice parameters may also indicate the oxygen vacancies which are usually created along with the incorporation of the impurity. The variation in the lattice constants clearly indicates the possibility of ${\rm Th^{4+}}$ ions substituting ${\rm Ti^{4+}}$ sites. Since the ionic radii of ${\rm Th^{4+}}$ (0.95 Å) ions is

much larger than Ti⁴⁺ (0.605 Å) it is quite unlikely that Th can act as substitutional impurity. For steric reasons however, the formation of complex defect comprising a Th atom and an oxygen vacancy in close proximity should be energetically more favorable. In Kröger and Vink notation, the probable chemical reaction can be represented in the following way.

$$ThO_2 \leftrightarrow Th_{Ti}^{-1} + V_0^{-1} + O_0 + 1/2 O_2 + 2e^{-1}$$

Where $Th_{\pi^{\parallel}}$ is Th ion at Ti lattice site with deficiency of one charge, V_0 doubly ionized oxygen vacancy, O_0 oxygen ion in a normal lattice site as proposed by Kofstad the defect equilibria in which the concentration of intrinsic defect (Oxygen vacancy) becomes equal to the concentration of extrinsic impurity.

3.1.4. Scanning Electron Microscope (SEM)



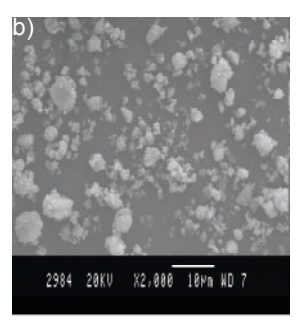


Figure 4. The SEM micrographs of ${\rm TiO_2}$ and ${\rm Th\text{-}doped\ TiO_2}$ (a) ${\rm TiO_2}$ (b) 0.06% ${\rm Th\text{-}doped\ TiO_2}$

The texture and morphology of the ${\rm TiO_2}$ and ${\rm Th\text{-}doped}$ titania surfaces are very important parameters and will influence the photocatalytic activity. The SEM image of 0.06% ${\rm Th\text{-}doped}$ ${\rm TiO_2}$ possesses porous and spongelike network of high roughness and complexity (Fig. 4). This results in a high surface area. It was also observed that particle size decreased after ${\rm Th}$ incorporation into ${\rm TiO_2}$ lattice, which results in the increase in the surface area of the modified doped systems.

3.1.5. Energy Dispersive X-ray Analysis (EDX)

The compositions of the different atom % of Th-doped ${\rm TiO_2}$ were determined using EDX analysis (Table 3). The analysis of the prepared samples clearly indicates the incorporation of Th which can be successfully achieved by the solid-state reaction.

The theoretical atom percentage of all the doped samples were calculated by using the relation

Atom % =
$$\frac{\text{No. of atoms of respective element}}{\text{Total no. of atoms}} \times 100$$

For 0.02% Th-doped sample $(Ti_{0.98}Th_{0.02}O_2)$

Atom
$$\% = \frac{\text{No. of atoms of respective element}}{\text{Total no. of atoms}} \times 100$$

Table 2. Calculated structural parameters of TiO₂ and different %Th-doped TiO₂ catalysts from XRD. The unit cell parameter is represented along with the standard deviation.

Catalyst	2 θ	d _{hki}	Unit Cell parameters (Å)	Unit cell Volume(Å)³	Crystal structure	Crystallite Size (nm)	Density g cm ⁻³
	05.4	0.510	0.7007 . 0.0010				
	25.4	3.513	3.7827 ± 0.0012				
TiO ₂	37.8	2.375	3.5459 ± 0.0008	143.630	Tetragonal	26.25	3.694
	48.1	1.891	10.7080 ± 0.0018				
	25.3	3.515	3.7822 ± 0.0006				
0.02% Th TiO ₂	37.8	2.376	3.7701 ± 0.0008	135.876	Tetragonal	26.27	3.707
2.22,2 2	48.1	1.891	9.5293 ± 0.0016				
	25.3	3.512	3.7824 ± 0.0012				
0.04% Th TiO ₂	37.8	2.378	3.7614 ± 0.0008	134.608	Tetragonal	26.28	3.758
	48.1	1.892	9.5142 ± 0.0016				
	25.0	0.540	0.7050				
	25.3	3.516	3.7856 ± 0.0012				
0.06% Th TiO ₂	37.8	2.378	3.7887 ± 0.0008	136.432	Tetragonal	26.29	3.894
	48.07	1.892	9.5123 ± 0.0016				
	25.32	3.516	3.7843 ± 0.0012				
0.1 % Th TiO ₂	37.8	2.376	3.7945 ± 0.0008	135.780	Tetragonal	32.28	3.917
	48.08	1.892	9.5058 ± 0.0016				

Therefore:

Atom % of Ti =
$$\frac{0.98}{1}$$
 × 100 = 98 %
Atom % of Th = $\frac{0.02}{1}$ × 100 = 2 %

Table 3. EDX data for TiO₂ and different atom % of Th-doped TiO₂

		Con	nposit	ion Ato	m, %
SI.No	Catalyst	Theor	etical	Experi	mental
		Ti	Th	Ti	Th
1	TiO ₂	100	-	100	-
2	0.02% Th-doped TiO ₂	98.0	2.0	97.87	2.13
3	0.04 % Th-doped TiO ₂	96.0	4.0	95.6	4.4
4	0.06% Th-doped TiO ₂	94.0	6.0	94.12	5.88
5	0.1% Th-doped TiO ₂	90.0	10.0	88.98	11.02

3.1.6. Multipoint BET adsorption

The nitrogen adsorption–desorption curve shows the characteristic type II isotherms (IUPAC classification) with small hysteresis loop. The surface area values are slightly higher for Th-doped samples. Specific surface area, total pore volume, and average diameter of modified ${\rm TiO_2}$ are summarized in Table 4. It can be observed that the surface area and average diameter

of the TiO₂ photocatalyst increases with the introduction of Th into the TiO₂ lattice, whereas the pore volume decreases. Therefore it can be inferred that when Th is incorporated, the metal is homogeneously distributed in the system without occupying the surface vacant sites

Table 4. Surface area, pore volume and average diameter of the TiO₂ and Th-doped TiO₃

SI.No	Sample	Specific surface area (m² g-1)	Total pore volume (cm³ g-1)	Average diameter (Å)
1	TiO ₂ (Anatase)	18.0	0.1859	89.175
2	Th-doped TiO ₂	20.69	0.0574	111.022

3.2. Photocatalytic activity of ${\rm TiO_2}$ and ${\rm Th\text{-}doped}$ ${\rm TiO_2}$

3.2.1. Degradation of OZ using ${\rm TiO_2}$ and ${\rm Th\text{-}doped\ TiO_2}$ under UV illumination

The extent of degradation of the pesticide is studied by withdrawing samples for analysis at any desired time interval during the reaction. The residual concentration of the pesticide was estimated from the standard calibration curves of absorbance vs. concentration of pesticide at particular value of λ_{max} 243 nm. Fig. 5 is the plot of pesticide concentration vs. the irradiation time for different experimental conditions, where 'C₀' is the initial concentration and 'C' is the residual concentration

of the pesticide at any time interval. From the figure it can be observed that photodegradation of OZ could not occur in aqueous solutions with only UV-light. Degradation is negligible even after three hours of UV-illumination in the absence of catalyst and oxidizing agent (curve 'a') which indicates that direct photolysis is a minor degradation pathway. The presence of only photocatalyst showed very slow rate of degradation (curve b). Oxidizing agents are thought to act as electron acceptors. These acceptors are known to enhance the generation of hydroxyl radicals which are thought to be the primary oxidizing species. They react rapidly with the aromatic hydrocarbons to yield hydroxylated adducts and subsequent reaction of these adducts can lead to the mineralization of the pesticide. The oxidizing agent used in the present research study is 5 mL of 0.001M (NH₄)₂S₂O₆ (optimum amount). The same concentration of oxidizing agent is used in all the experiments. There is a steep decrease in the concentration of pesticide within a short span of irradiation (2 hours) on addition of (NH₄)₂S₂O₈ along with the photocatalysts (curve 'c'). There is a decrease in photocatalytic efficiency when Th doped TiO2 is used as the photocatalyst under UV light (curves d, e, f, and g). This decrease could be explained on the basis of rate of generation of conduction band electrons and valence band holes and their life time. Usually electron hole recombination drastically lowers the rate of degradation. The estimated duration for electron trapping is 10 nanoseconds and hole trapping is 100 picoseconds. In the Th ion doped TiO2, the mid band gaps created due to the doping may act as recombination centers under UV light [39]. The relative

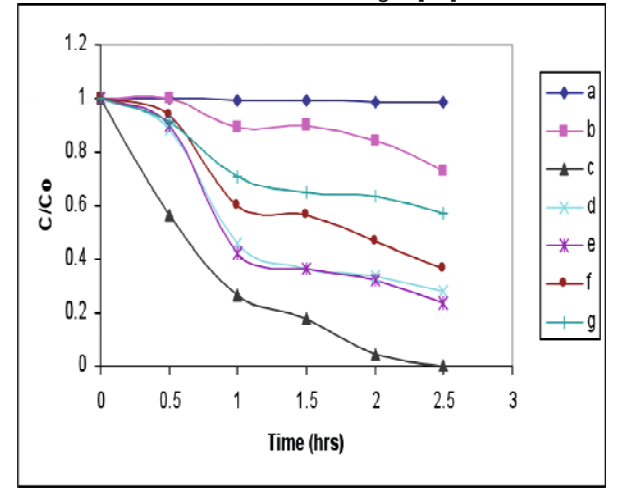


Figure 5. Plot of pesticide concentration $\mathrm{C/C_0}$ v/s the irradiation time under UV light illumination (a) only pesticide solution under UV light, (b) pesticide with only $\mathrm{TiO_2}$, (c) pesticide solution with $\mathrm{TiO_2}$ in presence of $(\mathrm{NH_4})_2\mathrm{S_2O_8}$, (d) Pesticide solution with 0.02% Th-doped $\mathrm{TiO_2}$ in presence of $(\mathrm{NH_4})_2\mathrm{S_2O_8}$, (e) Pesticide solution with 0.04% Th-doped $\mathrm{TiO_2}$ and $(\mathrm{NH_4})_2\mathrm{S_2O_8}$, (f) Pesticide solution with 0.06% Th-doped $\mathrm{TiO_2}$ and $(\mathrm{NH_4})_2\mathrm{S_2O_8}$, (g) Pesticide solution with 0.1% Th-doped $\mathrm{TiO_2}$ and $(\mathrm{NH_4})_2\mathrm{S_2O_8}$

percentage of degradation of OZ with ${\rm TiO_2}$ and Th-doped ${\rm TiO_2}$ are summarized (Table 5).

In the present study of photodegradation of OZ using semiconductor particles as photocatalysts, quantum yield determinations are hampered by several complications most of which is due to light scattering and recombination of charge carriers. As an alternative, kinetic measurements can be used to evaluate reaction rate, order of the reaction, rate constant, and process efficiency.

The plot of $\ln \text{C/C}_0$ vs. time shows (data not shown) the dependency of logarithm of residual concentration of OZ on illumination time. The higher negative slope of line indicates the faster rate of degradation. This is observed for the reaction in which both the catalyst and oxidant were present and where fairly good linearity in the plot is observed, indicating that all the reactions followed the first-order kinetics. Under illumination with UV-light only an oxidant and TiO_2 are sufficient to most effectively decompose oryzalin but not Th-doped TiO_2 .

3.2.2. Degradation of OZ using TiO_2 and Th-doped TiO_2 under solar light illumination

The photodegradation experiments were also carried out under sunlight in order to understand the activity of Th-doped ${\rm TiO_2}$ catalysts in presence of an oxidant (0.001 M (NH $_4$)₂S₂O $_8$) (Fig. 6). 50% of degradation takes place in 2.5 hours with anatase form of ${\rm TiO_2}$ (curve h), in contrast to 100% degradation in 1.5 hours with 0.06% Th-doped ${\rm TiO_2}$ (curve k). The kinetic parameters and process efficiency under sunlight illumination is shown in the Table 6. The enhanced photocatalytic activity of

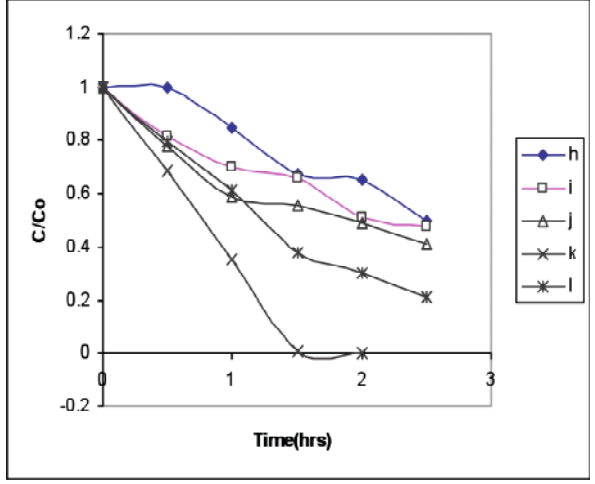


Figure 6. Plot of pesticide concentration $\mathrm{C/C_0}$ v/s irradiation time under solar light illumination (h) pesticide solution with $\mathrm{TiO_2}$ in presence of $\mathrm{(NH_4)_2S_0}_{\mathrm{Q_1}}$ (i) Pesticide solution with 0.02% Th-doped $\mathrm{TiO_2}$ in presence of $\mathrm{(NH_4)_2S_2O_8}$, (j) Pesticide solution with 0.04% Th-doped $\mathrm{TiO_2}$ and $\mathrm{(NH_4)_2S_2O_8}$, (k) Pesticide solution with 0.06% Th-doped $\mathrm{TiO_2}$ and $\mathrm{(NH_4)_2S_2O_8}$, (l) Pesticide solution with 0.1% Th-doped $\mathrm{TiO_2}$ and $\mathrm{(NH_4)_2S_2O_8}$

Table 5. The relative percentage of degradation of OZ with anatase form TiO_2/Th -doped TiO_2 in presence of ammonium persulphate as an oxidant under UV light for 2.5 hours. Process efficiency $\eta = (C_0-C)/t \times I \times S$, where C_0-C - decrease of pollutant concentration in mg L^1 , I - irradiation intensity in mw cm², S - the solution irradiated plane surface area in cm², t - the treatment time in hours)

SI. No	Catalyst (150 mg)	Oxidant (0.001M) (NH ₄) ₂ S ₂ O ₈	% degradation in 2.5 hours	Rate of reaction (hr-1)	Process efficiency (η) mg W ⁻¹ hr ⁻¹ cm ⁻²	Order of reaction	Rate Constant (-k) (hr ⁻¹)	Catalytic Coefficient (k C ⁻¹)
1			2	0.01	6.768×10 ⁻⁸	First	0.003	1.93c10 ⁻⁵
2	TiO ₂		27	0.22	7.897×10 ⁻⁷	First	0.054	3.6 ×10 ⁻⁴
3	TiO ₂	5 mL	100	0.95	5.785×10 ⁻⁵	First	1.845	12.3×10 ⁻³
4	0.02% ThTiO ₂	5 mL	72	0.86	4.734×10 ⁻⁵	First	0.477	3.1×10 ⁻³
5	0.04% ThTiO ₂	5 mL	77	0.85	4.972×10 ⁻⁵	First	0.386	2.5×10 ⁻³
6	0.06% ThTiO ₂	5 mL	64	0.66	3.716×10 ⁻⁵	First	0.345	2.3×10 ⁻³
7	0.1% ThTiO ₂	5 mL	43	0.42	8.800×10 ⁻⁷	First	0.132	8.8×10 ⁻⁴

Table 6. The relative percentage of degradation of OZ with anatase form TiO₂/Th-doped TiO₂ in presence of ammonium persulphate as an oxidant under solar-light for 2.5 hours.

SI. No	Catalyst (150 mg)	Oxidant (0.001M)	% degradation In 1.5 hours	Rate of reaction (hr ⁻¹)	Process efficiency (η) (×10 ⁻⁵) mg W ⁻¹ hr ⁻¹ cm ⁻²	Order of reaction	Rate Constant (-k) (hr ⁻¹)	Catalytic coefficient (k C ⁻¹)
1	TiO ₂	5 mL	50	0.35	2.9336	First	0.10933	0.0339
2	0.02%ThTiO ₂	5 mL	52	0.36	3.0706	First	0.13547	0.0420
3	0.04%ThTiO ₂	5 mL	59	0.38	3.4616	First	0.15358	0.0480
4	0.06%ThTiO ₂	5 mL	100	0.69	7.3340	First	0.47368	0.1470
5	0.1%ThTiO ₂	5 mL	78	0.47	4.6243	First	0.27298	0.0848

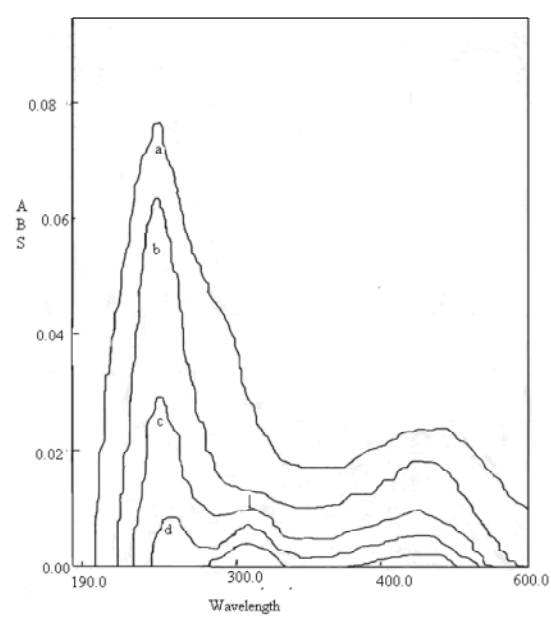


Figure 7. UV absorption spectra of the aqueous pesticide solution containing both an oxidizing agent $(NH_4)_2S_2O_8$ and photocatalyst under UV light illumination (a) 0 hours, (b) after 0.5 hours, (c) after 1.5 hour, (d) after 2.0 hours, (e) after 2.5 hours

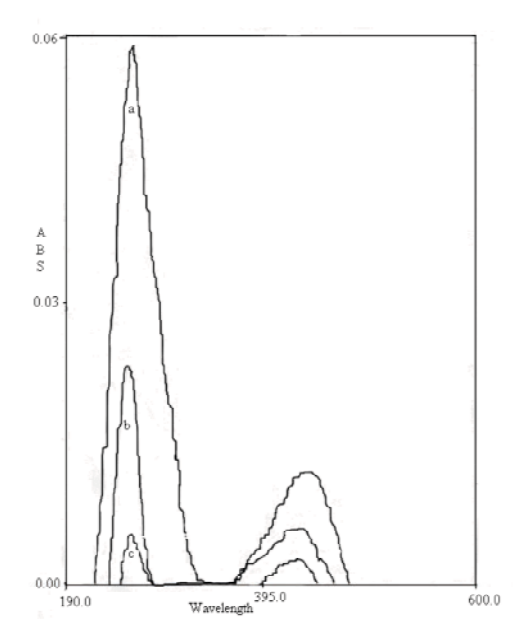


Figure 8. UV absorption spectra of the aqueous pesticide solution containing both an oxidizing agent $(NH_4)_2S_2O_8$ and photocatalyst under solar light illumination(a) 0 hours, (b) after 0.5 hours, (c) after 1.0 hour, (d) after 1.5 hours (absence of characteristic peaks confirms complete degradation)

Th-doped ${\rm TiO_2}$ can be accounted in the following way: (i) fast interfacial electron transfer rate due to creation of new energy levels at 2.84 eV, 2.804 eV, 2.66 eV, 2.55 eV from which an electron can be easily promoted to the conduction band, (ii) slow recombination of charge carriers (iii) ${\rm Th^{3+-V_0}}^{-}$ state acting as electron donor. The plot of logarithm of the pesticide concentration against irradiation time gives the kinetic order of degradation. Fairly good linear plots were observed, indicating that all reactions followed the first-order kinetics.

The following conclusions can be drawn from the above experimental results:

- 1. The presence of Th (in Th-doped ${\rm TiO_2}$) sample introduced a significant drop in band–gap energy from 3.12 eV to 2.55 eV which corresponds to radiation absorption at longer wavelength (\geq 486 nm). The decrease in Eg value may increase the absorption of visible solar light by the photocatalyst particles.
- 2. The incorporation of Th dopant is accompanied by the doubly ionized oxygen vacancy creating a donor level below the conduction band. The transition from this dopant level under visible light is most probable leading to the higher photocatalytic efficiency.
- 3. It is often observed that metal cation substitution in ${\rm TiO_2}$ induces the visible light activity but in most of the cases decreases its photoactivity under UV light. This may be due to the energy levels of the metal dopants located within the band gap could serve as recombination centers under UV- light.

3.3. Spectral Analysis of Reaction Intermediates

3.3.1. UV-Visible spectroscopy

Fig. 7 shows the UV-Visible spectrum of OZ taken at different time intervals for the reaction in which both photocatalyst and oxidizing agent is used under UV light. The initial curve (a) is taken before irradiation (UV/Solar) shows two prominent absorption bands at 244 nm and 440 nm. The peak at 244 nm is the E_a-band of substituted benzene and the substituted dialkyl amine acting as an auxochrome. The other prominent band at 440 nm is the B-band (benzenoid band) which is a characteristic peak of aromatic compounds. When chromophoric group is attached to an aromatic ring, the B-bands are observed at longer wavelengths than the more intense $\pi\to\pi^*$ transition (red shift). The B-band is expected to occur at 255 nm, but in OZ it appears at 440 nm due to the red shift. Due to two nitro groups at m-position, the peak shifts by (65 nm + 65 nm) 130 nm. The sulphonyl amide group at the m-position to the nitro group further shifts the peak by 55 nm. Therefore the peak appears at 440 nm instead of 255 nm. Substitution at meta position, shift effects are additive [40].

During the process of illumination, after one hour (curve c), a new peak appears at 320 nm. This may be due to the formation of dinitrophenol as an intermediate. The nitro phenol shows the B band at 280 nm. Due to the presence of another nitro group the peak appears at 320 nm. This confirms the dinitro phenol as the major intermediate during process of degradation under UV-illumination, which is further substantiated by GC-MS analysis.

Fig. 8 clearly indicates that dinitrophenol formation is a minor intermediate product under Solar light irradiation. Since the spectrum does not show any prominent change at 320 nm, the degradation mechanism may be slightly different between UV light and solar light illumination.

3.3.2. GC-MS Spectroscopy

The identified intermediates as proposed from UV analysis are further substantiated through mass spectral analysis. GC-MS spectra are taken for the samples extracted in to non aqueous chloroform at different time intervals of degradation for the efficient system. (10 mL of reaction mixture was extracted in 5 mL of chloroform. Further it is concentrated by evaporating the chloroform in the rotavaporizer. 1 µL of this sample was injected into GC-MS). The major high intensity peaks observed are at m/z = 346 (OZ) m/z = 263(4-hydroxy-3, 5-dinitrosulfanilamide), m/z = 184(3, 5- dinitrophenol), m/z = 167 (3, 5-dinitrobenzene). Very similar products were reported by Krieger et al. [41]. In addition to these major peaks there were several low intensity peaks at m/z values 246, 94, 78, etc. which may be identified as the intermediate products shown in the Scheme 2.

3.3.3. Proposed Probable Degradation Mechanism and the Reaction Intermediates

By observing the spectral changes that take place during the process of degradation and also depending on the source of irradiation, the following reaction mechanism has been proposed. Firstly the point of cleavage under UV light irradiation in presence of molecular oxygen is found to be between dialkyl amine and aromatic carbon leading to the formation of 4-hydroxy-3, 5-dinitrosulfanilamide. Further separation of sulphonyl amide group gives dinitrophenol (m/z = 184) in presence of hydrogen radical, and dintrophenol converts to Phenol (m/z = 94) followed by benzene as shown in Scheme 2. Based on these m/z values the probable degradation mechanism has been proposed. The peak positions of major intermediate products and the fragments are listed (Table 7).

Under the solar light illumination, the probable degradation path way may be slightly different as shown in the Scheme 2.

Scheme 2. Probable degradation mechanism of OZ both under UV and solar light illumination

4. Conclusions

Doping of Th into TiO, lattice was intended to modify the electronic properties of titanium dioxide photocatalyst, enabling the absorption of solar energy irradiation. The maximum permissible level of Th in TiO, lattice is found to be 0.06%. This concentration is within the dispersion capacity and does not modify the crystal structure. Since the structure shown in all the samples is anatase, with little modification in the lattice parameters. Various mid band gap states created are at 2.84 eV, 2.80 eV, 2.66 eV, and 2.55 eV. The mid band gap states may be assigned to Th3+-Vo. and Ti3+-Vo. The results obtained in the photocatalytic reactions were analyzed by UV-Visible and GCMS spectroscopic methods. These results indicate that Th-doped TiO, with the modified electronic properties is a good photocatalyst for the degradation of OZ in the surface water under solar light irradiation. But these modifications show very marginal differences in photocatalytic rates under UV-illumination. All the photodegradation reactions follow the first order kinetics. The major intermediate products formed during degradation process are m/z = 263(4-hydroxy-3, 5-dinitrosulfanilamide), m/z = 184 (3, 5- dinitrophenol), m/z = 167 (3, 5-dinitrophenzene).

Acknowledgements

Financial support by UGC-Major Research Project, UGC-DRS, and UGC-FIST is greatly acknowledged. One of the authors, B.Narasimha Murthy, wishes to acknowledge CMR Institute of Technology, Bangalore for its support.

Table 7. The peak positions of major intermediate products and the fragments

	UV Light Illuminated		Solar Light Illuminated
m/z	Intermediatecompond	m/z	Intermediate compound
263	O_2N NO_2 SO_2NH_2	246	O ₂ N NO ₂ SO ₂ NH ₂
84	O ₂ N OH NO ₂	166	O_2N NO_2
94	OH	78	
78			

References:

- [1] R.T. Meister, Farm Chemicals Handbook '92 (Meister Publishing Company, Willoughby, 1993)
- [2] Occupational Health Services, Inc. 1992 Nov. 17. MSDS for ORYZALIN (OHS Inc., Secaucus, 1992)
- [3] U. S. Department of Agriculture, Soil Conservation Service. 1990 Nov. SCS/ARS/CES Pesticide Properties Database: Version 2.0 Summary. USDA - Soil Conservation Service, Syracuse, NY
- [4] WSSA Herbicide Handbook Committee, Herbicide Handbook of the Weed Science Society of America, 6th edition (WSSA, Champaign, 1989)
- [5] U.S. Environmental Protection Agency, June 30, 1987, Pesticide Fact Sheet Number 211: ORYZALIN. US EPA, Office of Pesticide Programs, Registration Div., Washington, DC.
- [6] U.S. Environmental Protection Agency, June 20, 1990, Pesticide tolerance for Oryzalin. Federal Register 55 119: 25140-1
- [7] British Crop Protection Council, The Pesticide Manual: A World Compendium, 7th edition (Croydon, England. 1983)
- [8] U.S. Environmental Protection Agency, Nov. 21, 1984, Tolerances and exemptions from tolerances for pesticide chemicals in or on raw agricultural commodities; Oryzalin. Federal Register 49 (226): 45854-5
- [9] Washington State Department of Transportation, Roadside Vegetation Management: Environmental Impact Statement, WSDOT (1993)
- [10] Elanco Chemical Company, Summary of Basic Data for Oryzalin Herbicide, Elanco Products Co. (MSDS, Indianapolis, 1989)
- [11] R.D. Wauchope, T.M. Buttler, A.G. Hornsby, P.W.M.Augustijn Beckers, Burt, J.P.; SCS/ARS/CES, Rev. Environ. Contam. Toxicol. 123 1-157 (1992).
- [12] M.D. Bethesda, U.S. National Library of Medicine, Hazardous Substances Data bank, 9-10 (1995)
- [13] E. Borgarello, J. Kiwi, M. Gratzel, E. Pelizzetti, M. Viscald, J. Am. Chem. Soc. 104, 2996 (1982)
- [14] E. Pelizzetti, N. Serpone, eds, Homogeneous and Heterogeneous photocatalysis (Reidel, Dordtecht, 1986)
- [15] M. Schiavello, ed., Photocatalysis and Environment: Trends and Applications (Kluwer Academic publishers, Dordrecht, 1988)
- [16] E. Pelizzetti, N. Serpone, eds, Photocatalysis: fundamental and Applications (Wiley, New York, 1989)
- [17] J. Soria, J. C. Conesa, V. Augugliaro, L. Palmisano, M. Schiavello, A. Sclafani J. Phys. Chem. 95, 275 (1991)

- [18] N. Serpone, D. Lawless, Langmuir 10, 643 (1994)
- [19] W. Choi, A. Termin, M.R. Hoffmann, J. Phys. Chem. 98, 13669-13679 (1994)
- [20] H.Yamashita, H. Nishiguchi, N. Kamada, M. Anpo, Y. Teraoka, H. Hatano, S. Ehara, K. Kikui, L. Palmisano, A. Sclafani, M. Schiavello, M.A. Fox, Res. Chem. Intermediates. 20, 815 (1994)
- [21] Y, R. Do, W. Lee, K. Dwight, A. Wold, J. Solid State Chem. 108, 198 (1994)
- [22] J. Papp, S. Soled, K. Dwight, A. Wold, Chem. Mater. 6, 496 (1994)
- [23] G. Marcì, L. Palmisano, A. Sclafani, A.M. Venezia, R. Campostrini, G. Carturan, C. Martin, V. Rives, G. Solana, J. Chem. Soc., Faraday Trans. 92, 819 (1996)
- [24] C. Martín, G. Solana, V. Rives, G. Marcì, L. Palmisano, A. Sclafani, Catalysis Letters 49, 235 (1997)
- [25] M. Takeuchi, H.Yamashita, M. Matsuoka, M. Anpo,T. Hirao, N. Itoh, N. Iwamoto, Catalysis Letters 67,135 (2000)
- [26] L. Gomathi Devi, G.M. Krishnaiah, Journal of Photochemistry and photobiology A: Chemistry 121, 141 (1999)
- [27] Y. Suda, H. Kawasaki, T. Ueda, T. Ohshima, Thin solid films 453, 162 (2004)
- [28] B.Wawrzyniak, A. Morawska, B. Tryba, International Journal of Photoenergy 2006, 1 (2006)
- [29] J.D. Lee, Concise Inorganic Chemistry, 5th edition (Chapmann and Hall publication, London, 1996)
- [30] K. Prasad, A.R. Bally, P.E. Schmid, F. Lévy, J. Benoit, C. Barthou, P. Benalloul, Jpn. J. Appl. Phys. 36, 5696 (1997)
- [31] T.R.N. Kutty, P. Murugaraj, N.S. Gajbhiye, Mater. Lett. 2, 396 (1984)
- [32] T.R.N. Kutty, P. Murugaraj, N.S. Gajbhiye, Mater. Res. Bull. 20, 565 (1985)
- [33] T.R.N. Kutty, L. Gomathi Devi, Mater. Res. Bull. 20, 793 (1985)
- [34] M.P. Fuller, P.R. Griffiths, Analytical Chemistry 5013, 1906 (1978)
- [35] M. Cardona, G. Harbeke, Phys. Rev. 137A, 1467 (1964)
- [36] N.F.M. Henry, K. Lonsdale, Eds.; International Tables for X-ray Crystallography Vol.1 (Kynoch press, Birmingham, 1952)
- [37] L.D. Dong, J. Phy. Chem. B 104, 78 (2000)
- [38] B.D. Cullity, Elements of X-ray Diffraction (Addison-Weseley Publishing Co., Reading, MA, 1978) 140
- [39] H.P. Maruska, A.K. Ghosh, Solar Energy Mater. 1, 237 (1979)

- [40] R. Silverstein, G. Bassler, T. Morrill, Spectroscopic Identification of Organic Compounds, 4th edition (Wiley, New York, 1981)
- [41] M.S. Krieger, D.A. Merritt, J.D. Wolt, V.L. Patterson, J. Agric. Food Chem. 46, 3292 (1998)